Nuclear Inst. and Methods in Physics Research, A 928 (2019) 37–42

Contents lists available at ScienceDirect

Nuclear Inst. and Methods in Physics Research, A

journal homepage: www.elsevier.com/locate/nima

Accurate and informative analysis of positron annihilation lifetime spectra by using Markov Chain Monte-Carlo Bayesian inference method

B.C. Gu [a,b], W.S. Zhang [c,*], J.D. Liu [a,b], H.J. Zhang [a,b], B.J. Ye [a,b,**]

[a] State Key Laboratory of Particle Detection and Electronics, University of Science and Technology of China, Hefei 230026, China
[b] Department of Modern Physics, University of Science and Technology of China, Hefei 230026, China
[c] Network Information Center, Supercomputing Center, University of Science and Technology of China, Hefei, 230026, China

ARTICLE INFO

Keywords:
Positron annihilation lifetime spectra
Analysis programs
Markov chain Monte Carlo

ABSTRACT

Positron annihilation lifetime (PAL) spectroscopy is one of the most powerful methods to quantitatively characterize atomic-scaled lattice imperfections in condensed materials. Generally, one needs to fit a PAL spectrum by solving a local non-linear optimization problem which is more or less affected by initial guesses. Therefore, by using a traditional analysis program for the same PAL spectrum, different results with close goodnesses of fits are yielded by different researchers. Thus, it is difficult to judge the qualities of different results. To overcome this shortage, an efficient Markov Chain Monte-Carlo Bayesian Inference (MCMC-BI) method based on CosmoMC package is applied to analyze both simulated and experimental PAL spectra in the present work. The same level of accuracy of traditional analysis programs is firstly acquired in this work by using MCMC-BI method, which demonstrates that it can be directly used to analyze PAL spectra. Furthermore, the dependence on the initial guesses of PAL analysis is significantly alleviated. Additionally, more precious information is provided by MCMC-BI method, including different lifetime uncertainties in different confidence intervals and the correlations between annihilation parameters.

1. Introduction

Positron annihilation lifetime (PAL) spectroscopy is a state-of-art method to study the vacancy-type defects in condensed materials such as semiconductors, metals, and polymers, etc [1–4]. After implantation into a material from the positron source, the positrons firstly thermalize (lose kinetic energy through collisions with atoms) in a few picoseconds and then diffuse in the material prior to the eventual annihilation with electrons. Due to the relatively long half-life of 2.6 years and the practically simultaneously emitting of a 1.275 MeV γ-ray, ^{22}Na source is usually utilized as the positron source for PAL experiments. By measuring and analyzing the positron annihilation lifetime (the time interval between the start signal (1.275 MeV γ-ray) and the stop signal (the resulted 0–511 keV γ-rays) of a positron–electron pair), the precious information on the local electron density and atomic structure of the sample could be characterized.

To analyze an experimental PAL spectrum, it is a central and vital task to extract physically meaningful parameters. A PAL spectrum which consists of several decaying exponentials convoluted with the time resolution function of the PAL measurement system, could be written as a histogram $N(t)$ [5]. A PAL spectrum $N(t)$ can be written in the form of:

$$N(t) = \sum_{j=1}^{k_0} [A_j \exp(-t/\tau_j)] \otimes R(t) + B \tag{1}$$

where t, k_0, R, B, τ_j, A_j are the time, number of lifetime components, time resolution function, background, mean lifetime of the jth component, and a pre-exponential factor ($A_j\tau_j$ is the "area" of the lifetime component), respectively. Here, R is given by a sum of weighted Gaussians (k_p is set to 1 to simplify the computing in this work) which may be displaced with respect to each other. The time resolution function $R(t)$ of the PAL system is usually written as:

$$R(t) = \sum_{p=1}^{k_p} \omega_p G_p(t) \tag{2}$$

where ω_p is the weight, and $G_p(t)$ is defined as:

$$G_p(t) = \frac{1}{\sqrt{2\pi}\sigma_p} \exp\left(-\frac{(t - T_0 - \Delta t_p)^2}{2\sigma_p^2}\right) \tag{3}$$

* Corresponding author.
** Correspondence to: Department of Modern Physics, University of Science and Technology of China, 96 Jinzhai road, Hefei, AnHui, China.
E-mail addresses: wszhang@ustc.edu.cn (W.S. Zhang), bjye@ustc.edu.cn (B.J. Ye).

https://doi.org/10.1016/j.nima.2019.02.056
Received 6 August 2018; Received in revised form 18 February 2019; Accepted 20 February 2019
Available online 28 February 2019
0168-9002/

Here, T_0 represents the time-zero channel number (start channel) which is used as a reference, σ_p is the standard deviation, and Δt_p is a displacement. The objective of the analysis is to extract the lifetimes τ_j and their weights of the components $A_j\tau_j$ (usually denoted as I_j) from the raw experimental spectra.

Great efforts were made in the past decades to develop a number of computer programs to analyze PAL spectra. Generally, the analyzing programs could be divided into two different approaches, the deconvolution approach (such as CONTIN [6,7] and MELT [8]) and fitting a theoretical model approach (such as POSITRONFIT [9] and the well-tested PATFIT [10,11], PALSfit [5,12]). Additionally, some programs such as LTv9 [13] and LT10 [14]) combine the two approaches. However, as a very ill-posed problem [8], analyzing a PAL spectrum is rather difficult, no matter which approach is adopted. The solution is usually a local optimum value which is ambiguous to some degree. This indicates that, a very small disturbance (such as random noise during the measurement) in the experimental data may induce a quite different set of results. Therefore the researchers have to decide which solution is the most reasonable. These uncertainties introduce more ambiguities to the experimental results during the data analysis. Even though various methods were harnessed to overcome these difficulties (fixing the number of components in PATFIT [11] and LTv9 [13], using Maximum entropy principle in MELT [8], or even using the artificial neural network [15]), the ambiguity is alleviated to some extent but can hardly be eliminated absolutely. Different results are obtained from different initial guesses for the fitting parameters.

In 2009, Pascual-Izarra and his cooperators developed a new PAL analysis program, the so-called PAScual program, by applying a very excellent fitting algorithm by means of simulated annealing (SA) and Markov Chain Monte-Carlo Bayesian Inference (MCMC-BI) method [16]. And then the program was applied successfully to some experiments [17,18]. Previous studies [19] also proved that by using MCMC-BI method it is possible to improve the performance of traditional method. However, in the PAScual program, the accuracy of global optimization method (using only the SA combining MCMC-BI method) to analyze PAL spectrum is not high enough. Thus the global optimization method is only used to find the region of the global optimum to eliminate the influences of the initial guess. So the potentials of MCMC-BI method still need to be further explored, and the analysis results of MCMC-BI method also need to be discussed in detail.

Inspired by PAScual program, in the present work we attempt to employ an efficient MCMC-BI method based on a widely used MCMC engine CosmoMC software package [20,21] to obtain a global optimal solution which is robust and almost independent from the initial guesses. Compared to previous works, we greatly improved the performance of the MCMC-BI method. The accuracy of MCMC-BI increased to the level of traditional programs such as LTv9 which enables it to be directly used to analyze PAL spectra. While due to the improvement in the accuracy, the more meaningful information of the annihilation parameters including the likelihood of every parameter located around the optimal region can also be obtained and analyzed. The results of several simulated and experimental PAL spectra are compared with those from well-tested program LTv9. The correlations between different parameters and the uncertainties in different confidence intervals are also discussed.

2. Theoretical models

2.1. Bayesian inference

Bayesian inference is a powerful tool to estimate parameters and compare models. The annihilation parameters are random variables $\boldsymbol{\theta}$, and an experimental spectrum is a data set $\boldsymbol{D}$. The conditional probabilities of the parameter sets $\boldsymbol{\theta}$ which are given by the experimental spectrum $\boldsymbol{D}$ (denoted as $p(\boldsymbol{\theta}|\boldsymbol{D})$), are known as posterior probabilities. For a given $\boldsymbol{D}$, the calculation of posterior probabilities enables us to quantify the probabilities of the unknown parameters $\boldsymbol{\theta}$. Namely, one can estimate $\boldsymbol{\theta}$ by calculating the posterior probabilities for all possible solutions in parameter space. From Bayes' theorem, the posterior probability can be written in the form of:

$$p(\boldsymbol{\theta}|\boldsymbol{D}) = \frac{p(\boldsymbol{D}|\boldsymbol{\theta})p(\boldsymbol{\theta})}{p(\boldsymbol{D})} \tag{4}$$

where $p(\boldsymbol{D}|\boldsymbol{\theta})$ is the likelihood probability which is the conditional probability of $\boldsymbol{D}$ for a given $\boldsymbol{\theta}$, $p(\boldsymbol{\theta})$ is the prior probability of the model that expresses the prior knowledge of $\boldsymbol{\theta}$ parameters prior to the observed data $\boldsymbol{D}$, $p(\boldsymbol{D})$ is the marginal likelihood (or model evidence) which is independent of other parameters. In this work, the prior probability represents only the boundaries of fitting parameters. Therefore, $p(\boldsymbol{\theta})$ is a uniform distribution in its parameter space, and $p(\boldsymbol{D})$ is regarded as a scaling constant. Eventually, we have to calculate the likelihood $p(\boldsymbol{D}|\boldsymbol{\theta})$.

For a PAL spectrum which is a histogram, the measurement of each channel is an independent measurement that following Poisson statistics. For a large number of events, Poisson distribution can be approximated by normal distribution. Then the likelihood $p(\boldsymbol{D}|\boldsymbol{\theta})$ can be written as:

$$p(\boldsymbol{D}|\boldsymbol{\theta}) = \frac{\exp(-\frac{1}{2}\chi^2)}{\prod_k \sqrt{2\pi N(k)}} \tag{5}$$

where

$$\chi^2 = \sum_k \frac{[N^{\theta}(k) - N(k)]^2}{N^{\theta}(k)} \tag{6}$$

$N^{\theta}(k)$ and $N(k)$ represent the number of counts in the kth channel of the theoretical spectra from a set of $\boldsymbol{\theta}$ parameters and from the experimental spectra, respectively.

For the analysis of PAL spectra, it is the main task to find the solutions which yield the largest posterior probabilities $p(\boldsymbol{\theta}|\boldsymbol{D})$ in parameter space. Noticing that the smaller χ^2 the larger likelihood $p(\boldsymbol{D}|\boldsymbol{\theta})$, χ^2 is selected as the objective function to represent the goodness of fit. Therein, the main task is to find the solutions with smaller χ^2 values in parameter space.

After the calculation of posterior probabilities, further inferences can be made. In the present work, we use posterior mean (expectation value) as the point estimation of parameters, which can be written in the form of:

$$\langle\boldsymbol{\theta}\rangle = \int p(\boldsymbol{\theta}|\boldsymbol{D})\boldsymbol{\theta}d\boldsymbol{\theta} \tag{7}$$

2.2. Markov Chain Monte-Carlo

It is an extremely tough work to calculate all solution points in a high-dimensional parameter space, because the computing time and storage requirements increase exponentially with increasing number of parameters. Practically, we are more interested in the results near the optimal solution rather than those far away from the optimum. Markov Chain Monte-Carlo (MCMC) is a useful method to deal with this problem [22,23]. By using the Markov chain mechanism, one can generate a chain of samples in a sample space where more samples are generated in the most important region. In other words, the samples are generated from target distribution ($p(\boldsymbol{D}|\boldsymbol{\theta})$ in this study). Here we use the Metropolis–Hastings algorithm [24,25] to generate a Markov Chain with its equilibrium distribution equates to the likelihood distribution $p(\boldsymbol{D}|\boldsymbol{\theta})$.

According to Metropolis–Hastings algorithm, assuming that we are proposed a movement from current state $\boldsymbol{\theta}$ to a new state $\boldsymbol{\theta}'$, the probability of accepting this movement is:

$$\mathcal{A}(\boldsymbol{\theta}', \boldsymbol{\theta}) = \min\left(1, \frac{p(\boldsymbol{\theta}'|\boldsymbol{D})}{p(\boldsymbol{\theta}|\boldsymbol{D})}\frac{q(\boldsymbol{\theta}|\boldsymbol{\theta}')}{q(\boldsymbol{\theta}'|\boldsymbol{\theta})}\right) \tag{8}$$

Table 1
The results of four simulated PAL spectra fitted by LTv9 program and MCMC-BI method. For MCMC-BI method, the posterior mean results are listed.

Spec.	Methods	FWHM (ps)	τ_1 (ps)	I_1 (%)	τ_2 (ps)	I_2 (%)	τ_3 (ps)	I_3 (%)
A	Simulation	150	200	50	400	30	1500	20
	LTv9	148.0	199.5 ± 0.6	48.4 ± 0.6	396.0 ± 7.6	30.8 ± 0.6	1499.2 ± 6.5	20.8 ± 0.3
	MCMC-BI	157.9 ± 1.7	200.9 ± 3.8	48.9 ± 2.2	400.3 ± 12	30.1 ± 2.1	1497.7 ± 7.8	21.0 ± 0.2
B	Simulation	150	200	85	400	13	1500	2
	LTv9	148.0	200.1 ± 1.2	84.6 ± 0.7	400.9 ± 5.2	13.2 ± 0.8	1435.0 ± 71	2.2 ± 0.2
	MCMC-BI	159.7 ± 1.3	200.0 ± 1.7	84.4 ± 1.4	398.6 ± 19	13.4 ± 1.5	1410.2 ± 48	2.2 ± 0.1
C	Simulation	250	200	50	400	30	1500	20
	LTv9	248.9	199.7 ± 5.4	48.6 ± 2.0	398.0 ± 15	30.6 ± 2.1	1505.0 ± 7.6	20.8 ± 0.9
	MCMC-BI	251.2 ± 2.3	202.7 ± 4.7	49.1 ± 2.5	398.7 ± 13	29.8 ± 2.4	1493.9 ± 7.7	21.1 ± 0.2
D	Simulation	250	200	85	400	13	1500	2
	LTv9	248.9	199.7 ± 0.7	84.2 ± 0.2	393.5 ± 14	13.6 ± 1.1	1415.0 ± 26	2.2 ± 0.1
	MCMC-BI	253.2 ± 1.8	200.8 ± 2.2	84.4 ± 1.9	393.9 ± 21	13.3 ± 1.8	1370.6 ± 46	2.3 ± 0.2

The other Simulation information: offset = 1024 channels, time calibration = 25.54 ps/channel, total counts = 2×10^6 for each spectrum, background = 100 counts with Poisson noise. The spectra are generated by a simple Matlab code. The code and generated spectra are provided as research data.

where $q(\theta'|\theta)$ is an arbitrary proposal density distribution (conditional probability of a proposed state θ' for a given θ). The choice of proposal density distribution greatly affects the efficiency of an algorithm. Generally, we propose a distribution similar with the shape of target distribution to get a higher acceptance probability. Besides, if one parameter correlates with another, proposing of longer steps along the degeneracy directions will also increase the acceptance rate. In this work, covariances between parameters are used to improve the efficiency of sampling. The great advantage of this method is that it scales approximately linearly with the number of parameters at its best. This enables us to calculate more parameters without significant adding of computational cost.

MCMC method is widely used in various fields such as cosmology [26]. CosmoMC is a publicly available Markov Chain Monte Carlo engine which has been successfully used to explore cosmological parameter space [20,27,28]. In this work, we apply MCMC algorithm based on CosmoMC to analyze PAL spectroscopy. Besides the marginalized distributions, this method provides the shape of full posterior.

3. Results and discussion

To verify the validity of MCMC-BI method, we generated a series of simulated spectra by computer. The four spectra which are labeled from A to D, are analyzed by MCMC-BI method and LTv9 program. After calculating the parameters (background B, start time T_0), we input all the lifetimes, intensities, and time resolution in full width at half maximum (FWHM) into MCMC-BI process. Therefore, the parameters of background B, start time T_0, and displacement Δt_p are not presented as the MCMC-BI results, even though they are calculated in this method. The fitting region of interest ranges from $C_{peak} - 3$ to $C_{peak} + 600$ (C_{peak} denotes the peak channel). The parameters and results are shown in Table 1.

In Table 1, spectra A and B are typical PAL spectra in solid materials. Accurate results are obtained by both methods. However, for a very small I_3 intensity of 2%, both programs underestimate τ_3. The mean results given by MCMC-BI method are almost the same as those given by LTv9, while the uncertainties of most parameters are slightly larger. This is most probably due to the calculation method of marginal posterior of MCMC-BI. To calculate one parameter, MCMC-BI method considers all the other parameters as random variables in global parameter space but not the local optimal values. Compared to LTv9, MCMC-BI slightly overestimate the FWHM.

However, for spectra C and D (FWHM of 250 ps), the accuracy of FWHM is greatly improved compared to that of spectra A and B, while the accuracies of other parameters remain nearly unchanged.

Table 2
The results of four simulated PAL spectra fitted by LTv9 program, the BI method of PAScual program, and MCMC-BI method. For MCMC-BI method, we list the posterior mean results.

Spec.	Methods	τ_1 (ps) I_1 (%)	τ_2 (ps) I_2 (%)	τ_3 (ps) I_3 (%)	τ_4 (ps) I_4 (%)
E	Simulation	100 25	250 25	600 25	1000 25
	LTv9	97.4 ± 4.4 23.6 ± 1.3	238 ± 14 25.5 ± 0.7	593 ± 21 26.0 ± 0.6	1001 ± 7 25.5 ± 0.9
	PAScual[BI]	96 ± 3 23.5 ± 0.9	238 ± 5 25.8 ± 1.1	597 ± 16 26.2 ± 0.8	1003 ± 8 24.6 ± 1.2
	MCMC-BI in this work	97.8 ± 1.3 23.7 ± 0.8	240.8 ± 7.1 25.7 ± 0.4	603.2 ± 15.6 26.4 ± 0.5	1007 ± 7 24.2 ± 1.0
F	Simulation	150 50	250 50		
	LTv9	149.9 ± 4.5 48.8 ± 2.4	249.0 ± 3.5 51.2 ± 2.4		
	PAScual[BI]	144 ± 2 42.2 ± 2.1	243 ± 1 57.8 ± 2.1		
	MCMC-BI in this work	150.0 ± 2.6 49.6 ± 2.2	250.2 ± 2.3 50.4 ± 2.2		
G	Simulation	150 50	220 50		
	LTv9	149.3 ± 7.0 47.6 ± 5.5	218.5 ± 5.4 52.4 ± 5.5		
	PAScual[BI]	157 ± 5 58.5 ± 7.6	226 ± 6 41.5 ± 7.6		
	MCMC-BI in this work	149.6 ± 4.0 49.4 ± 5.2	220.3 ± 3.8 50.6 ± 5.2		
H	Simulation	150 50	190 50		
	LTv9	152 ± 18 50.1 ± 20.8	190 ± 15 49.9 ± 20.8		
	PAScual[BI]	142 ± 16 42.4 ± 23.8	189 ± 11 57.6 ± 23.8		
	MCMC-BI in this work	147.9 ± 6.8 47.1 ± 14.3	190.2 ± 6.3 52.9 ± 14.3		

The other Simulation information: FWHM = 270 ps, offset = 100 channels, time calibration = 58 ps/channel, total counts = 2×10^7 for spectrum E, and total counts = 2×10^6 for spectra from F to H, background = 100 counts. The generated spectra are provided as research data.

The estimation of FWHM is mostly determined by the region near the start channel T_0. For a larger FWHM value, it is much easier to

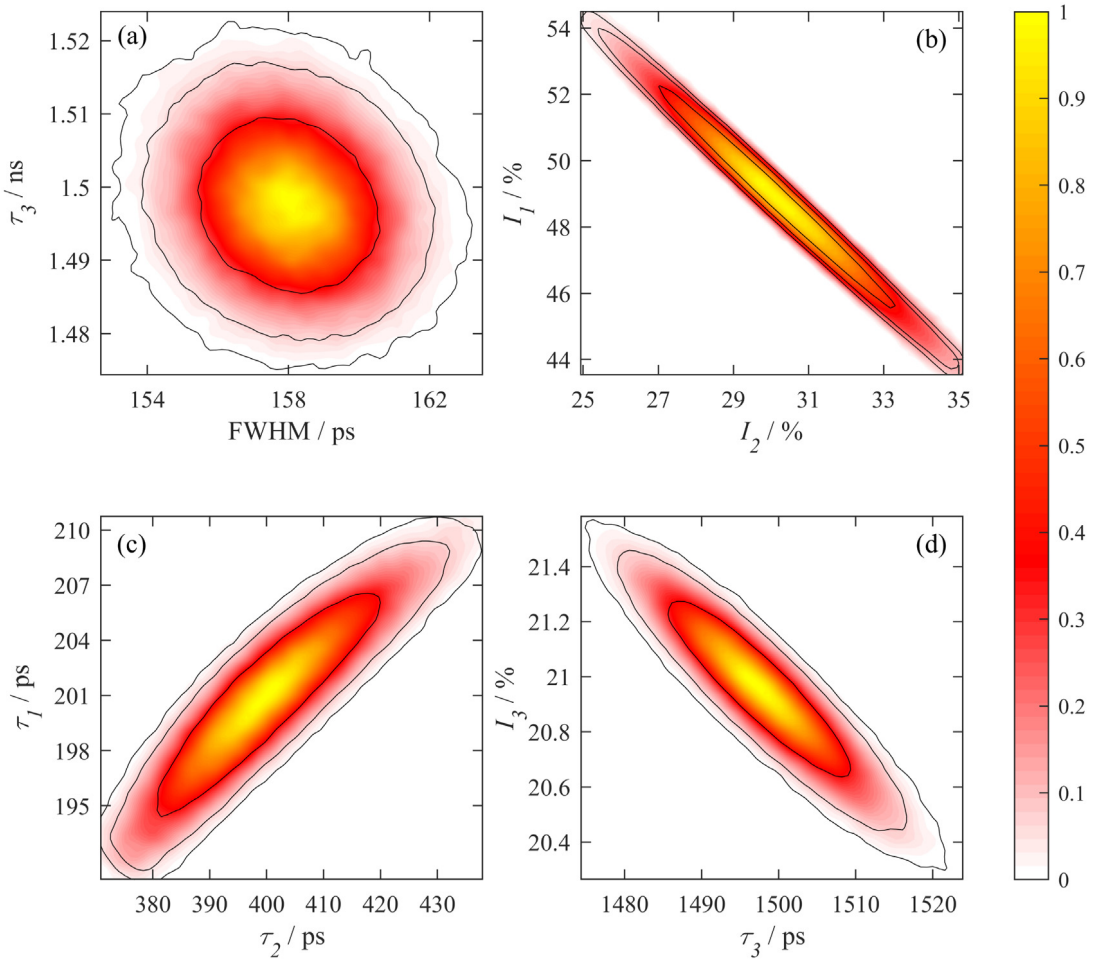

Fig. 1. Various posterior constraints of (a) (FWHM, τ_3) panel, (b) (I_2, I_1) panel, (c) (τ_2, τ_1) panel, and (d) (τ_3, I_3) panel near the optimal solution for spectrum A calculated by MCMC-BI method. In each subfigure, the three black contours are plotted to denote the 68%, 95%, and 99% confidence limits joint 2D marginalized contours. The intensity scale represents the normalized posterior distribution.

estimate FWHM using just several channels around the peak of spectra. Therefore, the selection of peak region may influence the estimation. The fitting results of spectra C and D (comparing with A and B, respectively) show that, the small deviation of FWHM affect slightly on the estimation of other annihilation parameters.

To compare PAScual program and MCMC-BI method, four spectra (E, F, G, and H) are generated by PAScual program at the same conditions in the previous articles [8,13,16]. The spectra have been analyzed by LTv9, PAScual, and MCMC-BI method. To make the comparison more relevant, in case of PAScual, the fit was performed using the global optimization BI method (the other global optimization methods including SA and SA + BI are also tested and the results are not significantly better than the BI method). The four simulated PAL spectra and their analysis results are shown in Table 2.

For spectrum E, the results of three programs are almost the same. All programs slightly underestimate τ_2 and I_1, but overestimate I_3. Spectra from F to H are generated to check the capability to distinguish the two lifetime components which are quite close to each other. With τ_2 diminishing from 250 ps (for spectrum F) to 190 ps (for spectrum H), the uncertainties from all programs increase significantly. Especially for the intensities of I_1 and I_2, the uncertainties increase drastically from less than 3% to nearly 20%. However, LTv9 and MCMC-BI are still able to give a relatively accurate answer, even for spectrum H (the posterior constraints results shown in Fig. S1 in the supplementary information). This evidently exhibits that LTv9 and MCMC-BI perform better than PAScual^{BI} on the estimation of intensities of I_1 and I_2. These analysis results also clarify that the performance of MCMC-BI method has been improved to the same accuracy level of LTv9.

The above analysis results demonstrate that, the MCMC-BI method is a feasible tool to provide a very accurate answer to the researchers. The accuracy of MCMC-BI method is comparable to those of traditional local optimization programs (such as LTv9). Furthermore, MCMC-BI could provide precious information on the probability distribution of all parameters. Because MCMC-BI method calculates plenty of possible solutions around the optimal solution, for each parameter we can get a visualized posterior constraint which represent the probability distribution. For all the simulated PAL spectra, we successfully acquired the posterior constraints of each parameter which confirmed that the mean solution is the corresponding global optimum of each parameter.

In Fig. 1 we show various posterior constraints of spectrum A near the optimal solution from a multi-dimensional (7-dimensional in this study) solution space. In each panel, the shading shows the posterior as a function of two different parameters, and the three black contours show the 68%, 95%, and 99% confidence limits from the marginalized distribution. Theoretically, in a long computing time the MCMC-BI method can always reach the global optimal solution not only the local ones. Compared to the results of traditional methods, the visualized solutions are able to illustrate whether there exists another local optimal solution around the best estimate results in the parameter space.

In the four subfigures of Fig. 1, the correlations between every two parameters are clearly illuminated. From Fig. 1a, it is obvious that FWHM is almost independent of the third lifetime component

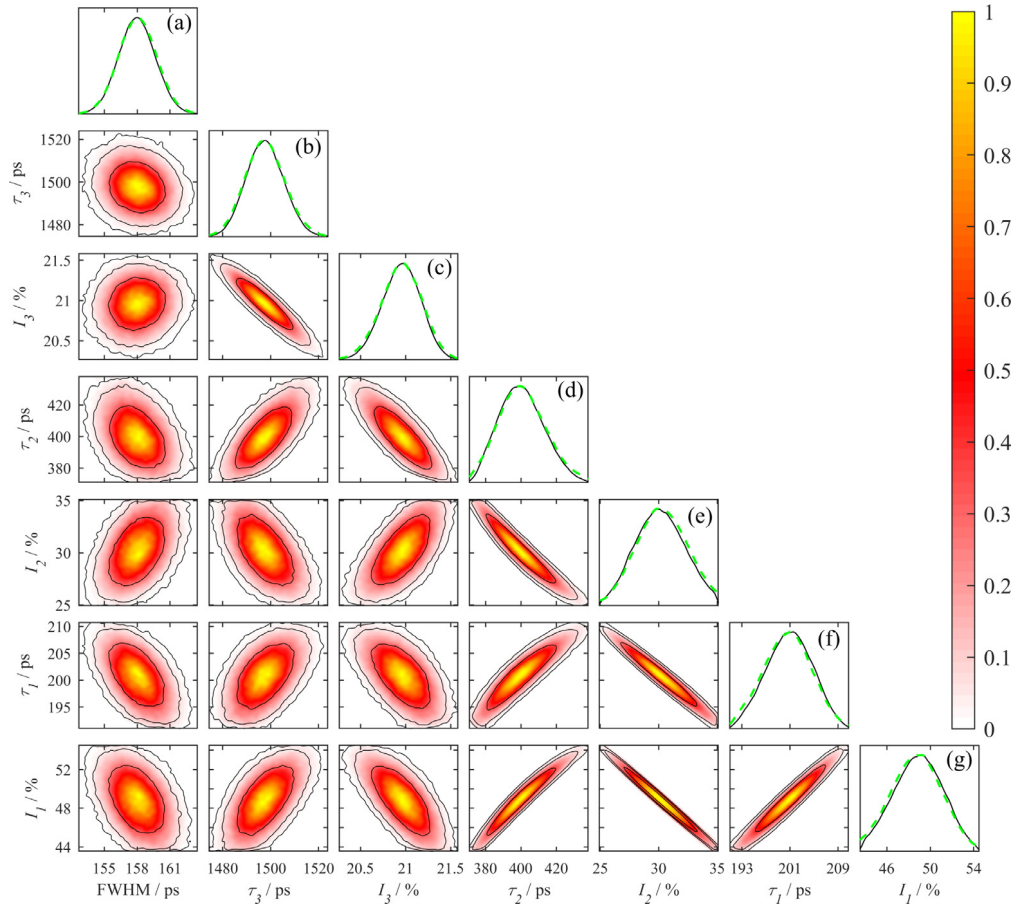

Fig. 2. Posterior constraints of all seven parameters near the optimal solution for spectrum A calculated by MCMC-BI method. The marginalized posterior probability (shown in black) and mean likelihood (shown in green) of all seven parameters are shown at the top of each column.

τ_3. So, it is reasonable that the fitted result of FWHM influences τ_3 slightly. Similar results can be found for other parameters (τ_1, τ_2, and etc.). On the contrary, as shown in Fig. 1b, the intensities of the first two lifetime components (I_1 and I_2) exhibit a very close correlation. According to Fig. 1b, if the user overestimates I_1, I_2 is more likely to be underestimated. In Fig. 1d, a similar tendency is also found for the correlation between the longest lifetime component τ_3 and its intensity I_3, although their correlation is relatively weaker. While on the other hand, the direction of the correlation between τ_1 and τ_2 is opposite to that of mentioned above, which shown in Fig. 1c.

This figure also explains why we should consider all parameters as variables but not a fixed optimal value to estimate the uncertainties. As shown in Fig. 1b, the 99% confidence interval of I_2 is around 10%. However, if we fix I_1 at its optimal value of 48.9%, all the three confidence intervals of I_2 decrease dramatically, even the 99% confidence interval is drastically reduced to around 1%. This suggests that MCMC-BI method which considers all parameters as random variables, is more comprehensive and informative for the calculation of standard deviation of each parameter. These results are necessary for users to understand the uncertainties more integrally and profoundly from another perspective.

Actually, the constraints of one parameter (of the 7 parameters) with another can be given, as shown in Fig. 2. It is clear that the correlations between FWHM and the other parameters are quite weak. This evidently explains that, the small deviation of FWHM can hardly influence the fitting of other parameters. At the top of all columns of Fig. 2, the posterior constraints of 7 parameters are plotted and denoted as (a)–(g). The black solid lines are the fully marginalized posteriors, while the green dashed lines represent the relative mean likelihoods of the samples. For Gaussian distributions, the black and green lines should be similar. While for skew distributions and the poorly converged chains, the black and green lines may be different [20]. The consistency of the marginalized posteriors and the mean likelihoods in this figure indicate that the MCMC chains are well converged. These curves show clearly the location of all optima and the types of distributions. And it is also evident that there is no other local optimum around the global optimal solution.

Finally, PAL measurements are performed for Si and GaN single crystals by using an ORTEC fast–fast coincidence system at room temperature. The time resolution of the system is about 230 ps in FWHM. A 20 μCi source of ^{22}Na is sandwiched between two identical sample pellets for measurements. Each spectrum is collected with a total count of 2×10^6. The experimental data are analyzed by MCMC-BI and LTv9 program.

The results of our experiments and other previous reports [29–33] are listed in Table 3. For the two single crystal samples, three lifetime components are observed. The first component τ_1 is the lifetime in the crystal, while τ_2 (around 380 ps) and τ_3 (around 2 ns) are regarded as source contribution. For Si and GaN, the lifetime τ_1 calculated by MCMC-BI agrees well with that obtained by LTv9 program, and with those from the literature.

In terms of usability, the MCMC-BI method based on CosmoMC in this work is not as convenient as the other widely used programs, since CosmoMC is coded in Fortran and requires Linux environment without a graphic interface for users. Instead of a user-friendly software as LTv9 and PAScual, it is more like a specialized package for calculation. A brief description of how to use CosmoMC is provided in the supplementary information.

Besides, unlike the local optimization methods such as LTv9 and PAScual^{LOCAL} which only take a few seconds to fit a spectrum, the

Table 3
The results of experimental PAL spectra for Si and GaN fitted by LTv9 and MCMC-BI (posterior mean results). The corresponding results in literature are also listed.

		LTv9	MCMC-BI		Ref	
Si	τ_1 (ps)	221.3 ± 1.3	220.2 ± 2.2	223 [29]	218 [30]	221 ± 1 [31]
	I_1 (%)	86.6 ± 0.1	87.5 ± 2.9	–	–	–
	τ_2 (ps)	384.5 ± 5.2	389.6 ± 19	–	–	–
	I_2 (%)	13.1 ± 0.1	12.0 ± 2.9	–	–	–
	τ_3 (ns)	2.3 ± 0.2	1.8 ± 0.2	–	–	–
	I_3 (%)	0.27 ± 0.02	0.47 ± 0.03	–	–	–
GaN	τ_1 (ps)	167.5 ± 0.3	168.7 ± 1.5	166 [32]	165 ± 1 [33]	–
	I_1 (%)	85.9 ± 3.7	87.3 ± 3.2	–	–	–
	τ_2 (ps)	376.0 ± 12	380.8 ± 22	–	–	–
	I_2 (%)	13.8 ± 3.7	12.3 ± 3.2	–	–	–
	τ_3 (ns)	2.0 ± 0.4	1.9 ± 0.3	–	–	–
	I_3 (%)	0.3 ± 0.07	0.37 ± 0.05	–	–	–

global optimization methods spend much longer time (highly depends on the number of samples) to calculate the posteriors. For PAScual[BI], it takes less than an hour to fit a spectrum, while for MCMC-BI in this work it takes relatively long time, around 3 h on a personal computer. The detail description about the time consumption is shown in the supplementary information see Fig. S2 and Fig. S3.

4. Conclusion

In summary, an efficient MCMC computer program has been employed to analyze PAL spectroscopy data. By using Markov Chain Monte-Carlo (MCMC) combining with Bayesian Inference, the program is directly utilized to analyze PAL spectra and provides a robuster and more reliable global optimal result which is almost independent of initial guesses. The reliability of MCMC-BI program has been tested by both simulated and experimental PAL data. Accurate mean results are achieved by using MCMC-BI method, which agree well with that of LTv9 program. On the other hand, the MCMC-BI approach yields more reasonable and slightly larger confidence intervals, and provides more visualized and detailed information to help us to avoid missing the global optimal solution. The correlations between every two parameters are found necessary to analyze the uncertainty of each parameter.

Acknowledgments

This work was supported by the National Natural Science Foundation of China (Grant No. 11475165, 11775215) and the Special Fund for Research on National Major Research Instruments, China (Grant No. 11527811).

Additional information

The authors declare no competing financial interests.

Appendix A. Supplementary data

Supplementary material related to this article can be found online at https://doi.org/10.1016/j.nima.2019.02.056.

References

[1] R. Krause-Rehberg, H.S. Leipner, Positron Annihilation in Semiconductors: Defect Studies, Vol. 127, Springer Science & Business Media, 1999.
[2] F. Tuomisto, I. Makkonen, Defect identification in semiconductors with positron annihilation: experiment and theory, Rev. Modern Phys. 85 (4) (2013) 1583.
[3] H.-E. Schaefer, Investigation of thermal equilibrium vacancies in metals by positron annihilation, Phys. Status Solidi (a) 102 (1) (1987) 47–65.
[4] Q. Deng, Y.C. Jean, Free-volume distributions of an epoxy polymer probed by positron annihilation: pressure dependence, Macromolecules 26 (1) (1993) 30–34.
[5] P. Kirkegaard, J.V. Olsen, M. Eldrup, N.J. Pedersen, PALSfit: a computer program for analysing positron lifetime spectra, in: Risø National Laboratory for Sustainable Energy, Technical University of Denmark, Roskilde, Denmark, Risø-R-1652, Citeseer, 2009.
[6] R.B. Gregory, Y. Zhu, Analysis of positron annihilation lifetime data by numerical laplace inversion with the program contin, Nucl. Instrum. Methods Phys. Res. A 290 (1) (1990) 172–182.
[7] R.B. Gregory, Free-volume and pore size distributions determined by numerical Laplace inversion of positron annihilation lifetime data, J. Appl. Phys. 70 (9) (1991) 4665–4670.
[8] A. Shukla, M. Peter, L. Hoffmann, Analysis of positron lifetime spectra using quantified maximum entropy and a general linear filter, Nucl. Instrum. Methods Phys. Res. A 335 (1–2) (1993) 310–317.
[9] P. Kirkegaard, M. Eldrup, Positronfit: a versatile program for analysing positron lifetime spectra, in: Tech. Rep., Danish Atomic Energy Commission Research Establishment, Risoe, 1972.
[10] P. Kirkegaard, M. Eldrup, O.E. Mogensen, N.J. Pedersen, Program system for analysing positron lifetime spectra and angular correlation curves, Comput. Phys. Comm. 23 (3) (1981) 307–335.
[11] P. Kirkegaard, N.J. Pedersen, M. Eldrup, et al., A data processing system for positron annihilation spectra on mainframe and personal computers, Riso Nat Lab Reports.
[12] J.V. Olsen, P. Kirkegaard, N.J. Pedersen, M. Eldrup, PALSfit: a new program for the evaluation of positron lifetime spectra, Phys. Status Solidi (c) 4 (10) (2007) 4004–4006.
[13] J. Kansy, Microcomputer program for analysis of positron annihilation lifetime spectra, Nucl. Instrum. Methods Phys. Res. A 374 (2) (1996) 235–244.
[14] D. Giebel, J. Kansy, Lt10 program for solving basic problems connected with defect detection, Physics Procedia 35 (2012) 122–127.
[15] A. Ran, Z. Jie, K. Wei, Y. Bang-Jiao, The application of artificial neural networks to the inversion of the positron lifetime spectrum, Chin. Phys. B 21 (11) (2012) 117803.
[16] C. Pascual-Izarra, A.W. Dong, S.J. Pas, A.J. Hill, B.J. Boyd, C.J. Drummond, Advanced fitting algorithms for analysing positron annihilation lifetime spectra, Nucl. Instrum. Methods Phys. Res. A 603 (3) (2009) 456–466.
[17] A.W. Dong, C. Pascual-Izarra, S.J. Pas, A.J. Hill, B.J. Boyd, C.J. Drummond, Positron annihilation lifetime spectroscopy (PALS) as a characterization technique for nanostructured self-assembled amphiphile systems, J. Phys. Chem. B 113 (1) (2008) 84–91.
[18] C. Pascual-Izarra, A.W. Dong, S.J. Pas, B.J. Boyd, C.J. Drummond, A.J. Hill, Advanced algorithms for PALS analysis of self-assembled amphiphiles, in: Materials Science Forum, Vol. 607, Trans Tech Publ, 2009, pp. 257–259.
[19] D. Ustundag, M. Cevri, U. Yahsi, Analysis of positron lifetime spectra using Bayesian inference, in: 2nd IET International Conference on Intelligent Signal Processing, 2015.
[20] A. Lewis, S. Bridle, Cosmological parameters from CMB and other data: A Monte Carlo approach, Phys. Rev. D 66 (10) (2002) 103511.
[21] A. Lewis, Efficient sampling of fast and slow cosmological parameters, Phys. Rev. D 87 (10) (2013) 103529.
[22] R.M. Neal, Probabilistic inference using Markov chain Monte Carlo methods, in: Technical Report CRG-TR-93-1, Department of Computer Science, University of Toronto, 1993.
[23] D. Gamerman, H.F. Lopes, Markov Chain Monte Carlo: Stochastic Simulation for Bayesian Inference, Chapman and Hall/CRC, 2006.
[24] N. Metropolis, A.W. Rosenbluth, M.N. Rosenbluth, A.H. Teller, E. Teller, Equation of state calculations by fast computing machines, J. Chem. Phys. 21 (6) (1953) 1087–1092.
[25] W.K. Hastings, Monte Carlo sampling methods using Markov chains and their applications, Biometrika 57 (1) (1970) 97–109.
[26] N. Christensen, R. Meyer, L. Knox, B. Luey, Bayesian methods for cosmological parameter estimation from cosmic microwave background measurements, Classical Quantum Gravity 18 (14) (2001) 2677.
[27] A. Hojjati, L. Pogosian, G.-B. Zhao, Testing gravity with CAMB and CosmoMC, J. Cosmol. Astropart. Phys. 2011 (08) (2011) 005.
[28] D.N. Spergel, R. Bean, O. Doré, M. Nolta, C. Bennett, J. Dunkley, G. Hinshaw, N.e. Jarosik, E. Komatsu, L. Page, et al., Three-year wilkinson microwave anisotropy probe (WMAP) observations: implications for cosmology, Astrophys. J. Suppl. Ser. 170 (2) (2007) 377.
[29] P. Sen, C. Sen, Effect of doping on positron lifetime in Si crystals, J. Phys. C: Solid State Phys. 7 (16) (1974) 2776.
[30] S. Dannefaer, P. Mascher, D. Kerr, Monovacancy formation enthalpy in silicon, Phys. Rev. Lett. 56 (20) (1986) 2195.
[31] S. Dannefaer, Defects and oxygen in silicon studied by positrons, Phys. Status Solidi (a) 102 (2) (1987) 481–491.
[32] K. Saarinen, T. Laine, S. Kuisma, J. Nissilä, P. Hautojärvi, L. Dobrzynski, J. Baranowski, K. Pakula, R. Stepniewski, M. Wojdak, et al., Observation of native Ga vacancies in GaN by positron annihilation, MRS Online Proceedings Library Archive 482.
[33] K. Saarinen, J. Nissilä, P. Hautojärvi, J. Likonen, T. Suski, I. Grzegory, B. Lucznik, S. Porowski, The influence of mg doping on the formation of Ga vacancies and negative ions in GaN bulk crystals, Appl. Phys. Lett. 75 (16) (1999) 2441–2443.